Temperature and volume dependence of the thermal conductivity of solid neon

H. T. Weston
AT&T Bell Laboratories, Murray Hill, New Jersey 07974

W. B. Daniels
Department of Physics, University of Delaware, Newark, Delaware 19711
(Received 7 October 1983)

The thermal conductivity κ of solid natural neon has been measured by the linear-flow method for specimens isobarically frozen from the dense-fluid phase within a high-strength steel cell. By crossing the fusion curve at several different pressures to as high as 7×10^3 bars, crystalline samples with molar volumes between 11.16 and 13.35 cm^3/mole were grown, and for each the isochoric variation of κ vs T was determined at a set of temperatures in the experimentally accessible range between 5 and 40 K. The large magnitude of κ and reproducibility of the results demonstrate that the present method of preparation and manipulation of solid neon consistently yields good-quality specimens. An analysis utilizing the zero-degree limit of the Debye temperature Θ_0 to account for all volume dependence indicates that the array of data, when expressed in terms of the resistive mean free path, may be rendered into a single function of the inverse reduced temperature Θ_0/T. The exponential variation of this common curve over more than 2 orders of magnitude is characteristic of three-phonon umklapp scattering and thereby gives support to Peierls's model of heat transport in dielectric crystals. More recent first-principles theoretical calculations are in qualitative agreement with experiment but yield conductivities somewhat below the observed values.

I. INTRODUCTION

In dielectric solids quantized lattice vibrations, or phonons, typically provide the dominant means for the transport of thermal energy, and it is momentum-nonconserving scattering of these phonons which leads to the dissipation of heat currents in such materials. The underlying source of resistive phonon scattering arises from the coupling of phonon states via lattice imperfections and/or anharmonicity of the interatomic potential. Information about these inherent mechanisms which affect the propagation of phonons in a solid may be obtained from an experimental determination of the thermal conductivity κ—a parameter which provides a quantitative measure of the impedance to heat flow.

The solidified inert gases are probably the simplest representatives of the solid state, and as such provide an excellent laboratory for the investigation of the lattice-dynamical properties of nonmetals. The interpretation of thermal-conductivity data should be easiest for measurements made on these substances since they so closely approximate the theoretically studied models of ideal crystals. Furthermore, the relatively large compressibility of the inert-gas solids enables one to constrain specimens within a high-strength-steel pressure vessel in such a manner that κ-vs-T data may be acquired under essentially constant volume conditions. In the absence of complicating thermal-expansion effects, the experimental results may then be directly compared with the predictions of various theoretical computations that have been developed in the Helmholtzian representation with temperature and volume serving as the independent variables. In addition, by performing measurements on samples of a gas solidified at a number of different molar volumes, the manner by which κ depends on v may also be inferred.

To date, it is only solid helium[1] and argon[2] that have been extensively studied to determine the volume as well as temperature dependence of their conductivities. Similar information about solid neon would also be desirable in order to make more complete the set of data available to the theorist on these simple systems. Although a few such measurements have been reported, they dealt with the low-temperature thermal conductivity of only modestly compressed neon specimens.[3] The present experiment, on the other hand, is concerned with an examination of the thermal transport behavior of neon over a broad range of molar volumes. Attention is directed principally to those temperatures where the dissipative phonon-phonon interactions of umklapp processes dominate.

II. EXPERIMENTAL DETAILS

For solid neon, with its fcc structure, the coefficient of thermal conductivity may be represented as a scalar quantity and may be determined as the constant of proportionality in the expression

$$\vec{Q}=-\kappa\vec{\nabla}T\ , \tag{1}$$

which relates the thermal energy current density $\vec{Q}$ to an imposed temperature gradient $\vec{\nabla}T$. This definition serves as the basis of the steady-state heat-flow method for measuring κ. It is a simple yet reliable technique and is most straightforward when applied to a linear sample of uniform cross section. The usual procedure calls for one end of the sample to be placed in contact with a thermal reservoir while the other end is electrically heated. Mea-

surement of the power input to the heater together with the cross-sectional area of the sample and the temperature difference between two points separated by a known distance along the axis of the sample then enables one to calculate the thermal conductivity directly using Eq. (1).

For the present study of a solidified gas at constant molar volumes, however, it is necessary to contain the specimens at high pressure and low temperature. This requires the use of a relatively thick-walled steel sample cell suspended from the thermostatically controlled tail of a liquid-helium cryostat. This mount serves as a heat sink for the thermal-energy current generated by the gradient heater attached to the closure end of the pressure cell. The basic experimental configuration is as shown in Fig. 1.

The details of this setup are dictated by several design criteria. For example, because of the need to withstand high internal pressures, the sample chamber is made from 18%-Ni maraging steel with yield strength of 2070 MPa. This alloy possesses outstanding strength and ductility characteristics even under cryogenic conditions. To ensure a bursting pressure greater than about 9×10^3 bars, and yet allow one to deal with reasonably sized specimens, the cell was fabricated with an inner diameter of 0.6356 cm and an outside diameter of 1.0266 cm. Although the ratio of outer to inner diameter is as small as is practicable, there is enough steel present that a significant fraction of the energy generated by the gradient heater is not transmitted through the sample, but is instead shunted to the cold block of the Dewar via the wall of the pressure cell. Since a quantitative measure of this proportion of heat carried by the wall is required for a proper computation of the thermal conductivity of any sample, it was first necessary to make an independent determination of the conductivity of the maraging steel alone. This was done by performing measurements on the evacuated cell at a series of temperatures in the experimentally significant region from 5 to 40 K. No data were collected at higher temperatures because the conductivity of the steel increases to such relatively large values that virtually all of the heat is transported by the cell wall, and the presence of the sample in its interior becomes nondetectable within the resolution of the instrumentation used. The radial flow technique used by Clayton and Batchelder is better adapted to high-temperature studies.[2]

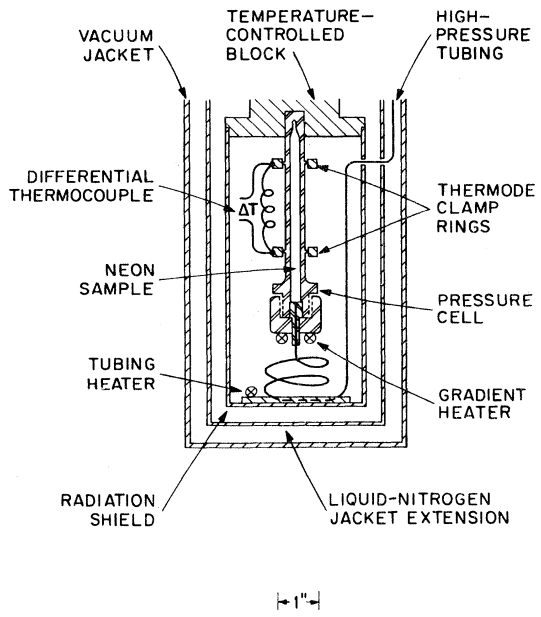

FIG. 1. Basic experimental configuration.

The principal thermometry components used to ascertain the temperature field distribution of the system are a germanium resistance element, needed for an absolute determination of T, and a differential thermocouple of Au + 0.03 at.% Fe and Cu construction. The latter device exhibits excellent thermoelectric sensitivity at low temperatures and, in conjuction with a dc potentiometer having a least-count equal to 10 nV, can directly measure a ΔT as small as 0.001 K. Since the temperature difference of interest is that across a given length of the sample, it is important that the measuring section be located near the central portion of the pressure cell where the surfaces of constant temperature are sufficiently planar that the gradient obtained at the exterior wall is identical to that which occurs in the specimen confined inside. It is for this reason that the cell has a rather long slender profile with the thermocouple junctions clamped to it at positions several diameters away from the complicated geometry near either end of the inner cavity.

The source of the heat flux through the experimental region is a 1500-Ω Nichrome resistor cemented to the bottom of the pressure cell. It is wired in series with a variable dc power supply along with a precision resistor which is used to monitor the current in the circuit. Typically, electrical energy supplied to the gradient heater at a rate less than a milliwatt is all that is required to maintain a ΔT between the thermocouple junctions on the order of 1% of the sample's average temperature. Nevertheless, an accurate determination of such low power dissipations is routine when the above-mentioned potentiometer is employed for the necessary voltage measurements.

Although the energy developed in the gradient heater is, for the most part, constrained to flow through the sample region, some fraction is conveyed away from the resistor by the electrical leads and pressure tubing. By utilizing long coiled lengths of fine gauge wire and 0.08-cm-o.d. capillary tubing, in conjunction with appropriate thermal anchoring of these components, it has been possible to reduce the calculated loss along their associated thermal paths to about one-third of one percent.

On the other hand, there may also be a contribution to the heat current through the sample region which is not due to the electrically generated power in the Nichrome heater, but instead arises from the unavoidable heat leaks into the low-temperature environment. The two principal mechanisms—thermal radiation and transport by the few molecules present in the imperfect vacuum envelope—are, however, not of major consequence in the present study. This is because the slight temperature difference between the experimental arrangement and the surrounding thermal shield allows for little radiative transfer, while the cryogenic pumping action of the cold hardware surfaces maintains an excellent vacuum so as to limit severely any

residual gas conduction or convection. Furthermore, so long as these unwanted heat inputs are not large and can be assumed independent of the small amounts of energy generated internal to the system, it is an easy matter to entirely eliminate their effect. This is done at any particular temperature by performing two sets of measurements, each for a different level of power dissipation in the gradient heater. Manipulation of the data so obtained then allows for the parasitic addenda to the heat current through the sample region to be canceled by means of a simple subtraction.

III. SAMPLE PREPARATION

The neon samples studied in this experiment were prepared from a 99.998% chemically pure natural isotopic mixture of approximately 91 at. % ^{20}Ne and 9 at. % ^{22}Ne. Each solid specimen of a particular molar volume v was formed by isobaric growth from the dense fluid melt at the appropriate point along the P-T fusion curve.[4] The growth conditions for the individual samples are shown in Table I.

The method calls first for the cell to be prepressurized at room temperature, in order to firmly seat its Teflon sealing gasket, and subsequently cooled to the desired neon freezing point $T_f(v)$, while manipulating the pressure in such a manner as to remain just on the fluid side of the fusion curve. Once at this point of $T=T_f(v)$ and $P \lesssim P_f(v)$, the 1500-Ω gradient heater is turned on and adjusted so that the bottom of the cell is maintained about 0.2 K warmer than the top. This helps ensure that the inlet to the cell is not closed off by frozen neon before the interior has been filled with solid. Likewise, premature blockage of the connecting capillary tubing is prevented with the use of a small resistor positioned at the tubing's thermal anchor to the heat-radiation shield.

The pressure in the system is then gradually increased until the onset of solidification occurs. This is manifested by a marked relaxation in pressure as recovery occurs from a superpressed state and the first bit of neon crystallizes into the nucleation tip at the top of the sample chamber. After the pressure has stabilized at $P=P_f(v)$, an overpressure of a few bars is again generated, which drives more fluid into the cell. As this additional neon solidifies, the pressure again drops back to the equilibrium freezing point at which time the sequence is repeated with the result that the horizontal interface between the coexisting solid and fluid phases slowly moves down the length of the cell. This inverted arrangement is intended to allow contaminants such as particles of dust, Teflon, etc., which may be suspended in the fluid neon to sink to the bottom of the cell before they can become incorporated as imperfections in the solid.

When the content of the pressure vessel cavity is entirely solid neon, the gradient and tubing heaters are deenergized. This results in a frozen plug of neon forming in the tubing entry so that the sample becomes isolated from the external pressure generating apparatus. Finally, an anneal for several hours is performed in an effort to reduce structural defects and the nonuniform density distribution in the solid. The latter is due to the slight variation in growth conditions along the small temperature gradient maintained across the length of the cell during the solidification process.

Once prepared in the above fashion, each specimen is cooled from its growth point down to the range of temperatures in which the thermal-conductivity measurements are to be performed. Here it is necessary to proceed very slowly in order to minimize thermal inhomogeneities and accompanying damaging pressure gradients. Even a difference in temperature of a few degrees between the ends of a sample can be sufficient to generate a pressure difference on the order of a hundred bars in such a clamped system.[5] Only by exercising care it is possible to reduce thermal shock to the samples and thereby prevent excessive stresses from developing across them.

Yet, because the pressure cell is not perfectly rigid, it is impossible to avoid introducing some strain into a specimen. The character of this deformation is chiefly a reduction in volume as the dimensions of the sample chamber diminish slightly with the decrease in internal pressure that occus when the temperature is lowered from the freezing point to the experimentally relevant region. The geometrical changes which occur in this manner have been calculated and are in every case less than about 0.5%. Furthermore, for each specimen studied, data are acquired sufficiently far below the fusion curve that thermal and elastic contractions have all but ceased before these low temperatures are attained. Indeed, the volume change over the temperature range in which a given sample's conductivity is measured is typically only about 0.1%, so that the data may be considered as being gathered under essentially isochoric conditions. Table I contains a listing of the low-temperature molar volumes for all the solid-neon specimens studied in this experiment. Also given, to aid the data analysis that follows, are the zero-degree Debye characteristic temperatures $\Theta_0(v)$ corresponding to these molar volumes.[6]

TABLE I. Summary of thermodynamic parameters for the experimental samples. The Debye temperatures are derived from the results of Fugate and Swenson (Ref. 6).

Sample	T_f (K)	P_f (bars)	$v(P_f,T_f)$ (cm^3/mole)	$v(P,T\gtrsim 0)$ (cm^3/mole)	$\Theta_0(v)$ (K)
Neon 1*A*, 1*B*	35.0	780	13.38	13.35	75.78
Neon 2	46.3	1810	12.70	12.66	86.58
Neon 3	62.8	3580	12.01	11.95	100.08
Neon 4	85.9	6480	11.24	11.16	118.82

IV. RESULTS

Because solid neon is a material for which some thermal-conductivity data already exist from several sources,[3,7,8] the initial effort of this experiment was to use some of these prior results as a benchmark for establishing the reliability of the present technique for determining κ. To this end, the first samples neon 1*A* and neon 1*B* were grown at such a point on the fusion curve that, when cooled at an almost constant volume of 13.35 cm^3/mole, their internal pressure declined to only a small positive value near 0 K. The conductivity values measured for these specimens could then be compared with the observations of Kimber and Rogers,[7] who worked with 13.39-cm^3/mole free-standing solids in equilibrium with their saturated vapor at $\simeq$1 bars. Joint consideration of these results is facilitated in Fig. 2 in which are presented the data of this study together with a smoothed curve representing the low-temperature findings of Kimber and Rogers. As can be seen, the results of these two investigations are in excellent agreement and support the validity of the present experimental method.

Kimber and Rogers report that they were able to form and maintain specimens which visual inspection revealed to have a good appearance with polycrystalline boundaries on the thermally etched surfaces separated by several millimeters or more. The comparable conductivity found for neon 1*A* and neon 1*B* of the present study indicates that their degree of perfection is similar to that of the Kimber and Rogers samples. It is reasonable to suppose this is true as well for our other samples having smaller molar volumes. Corroborative evidence for this assumption is given by the fact that similar specimens grown at high pressures for neutron scattering studies were also observed to have grains of large dimensions and a tight mozaic structure.[9–11]

As an indication of just how sensitive the low-temperature thermal conductivity is to sample quality, the results of White and Woods[8] are also graphically illustrated in Fig. 2. The disappointedly low κ values obtained by these investigators are acknowledged to be caused by the severely damaged condition of their specimens as the internal pressure became negative upon cooling and they tended to pull away from the walls of their Inconel container.

Lastly, in an attempt to learn something about the volume dependence of the conductivity, κ was measured as a function of temperature along several different isochoric traces. In addition to the measurements performed at 13.35 cm^3/mole, data were also acquired at three other smaller volumes (see Fig. 2). The final sample had a molar volume of 11.16 cm^3/mole in the temperature span of interest and was grown at 6480 bars. Preparation of specimens with suitably smaller molar volumes was not attempted because pressures exceeding the design criteria of the experimental cell would be required. Nevertheless, even within this limitation, it was possible to produce and thereupon study solid-neon samples with molar volumes differing by almost 20%.

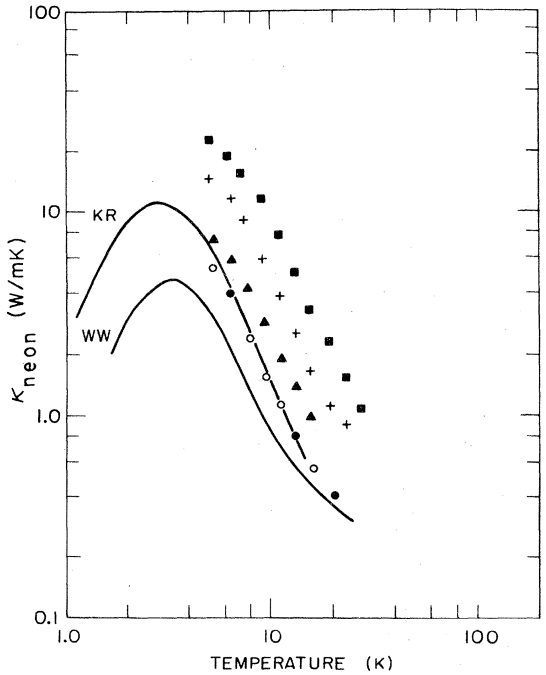

FIG. 2. Thermal conductivity of solid neon along several isochores. The present data are given by ○,●, neon 1*A*, 1*B* (13.35 cm^3/mole); ▲, neon 2 (12.66 cm^3/mole); +, neon 3 (11.95 cm^3/mole); ■, neon 4 (11.16 cm^3/mole). The smoothed results for the $\simeq$1 bars experiments of Kimber and Rogers (Ref. 7) and White and Woods (Ref. 8) are represented by the curves labeled KR and WW, respectively.

V. PHENOMENOLOGICAL ANALYSIS

Insight into the nature of the interaction mechanisms which impede the transport of heat in solid neon is facilitated if the data of Fig. 2 are discussed in terms of the free path between those phonon scattering events responsible for limiting the thermal conductivity κ. A convenient approach is to regard the phonons as constituents of a quasiparticle gas which pervades the crystal lattice. In this way, the desired mean free path l between collisions which retard the flow of heat may be associated with the measured values of κ by way of the simple relation

$$l=\frac{3v\kappa}{Cu}\ , \tag{2}$$

which is well known from the kinetic theory of gases. In this expression v represents the molar volume, C the specific heat capacity, and u an appropriately averaged velocity of sound.

Determination of the quantities C and u needed in the above formula is most easily performed within the framework of the Debye model.[12] For example, the heat capacity at constant volume in this context is given by

$$C_v=9Nk_B(T/\Theta)^3\int_0^{\Theta/T}x^4\exp(x)[\exp(x)-1]^{-2}dx\ , \tag{3}$$

with x being the reduced frequency $\hbar\omega_q/k_BT$, Θ is the Debye temperature, and N is Avogadro's number. Although not solvable in closed form, this integral can be numerically evaluated[13] at any desired reduced temperature T/Θ. Also, if no distinction is made between longi-

tudinal and transverse vibrational modes, the Debye first-sound velocity is described by the equation

$$u = k_B\Theta(v/6\pi^2\hbar^3N)^{1/3} . \quad (4)$$

In view of these approximations, the mean free paths arising from Eq. (2) will be only approximate, but nevertheless they may be expected to display the proper temperature and density behavior and be of the correct order of magnitude.

Conveniently characterizing each sample by the zero-degree limit of its Debye temperature, the calculated values of the mean free path l are exhibited in Fig. 3. A prominent feature of this graph is the manner whereby the matrix of data points is made to fall quite close to a common curve when temperature is normalized by Θ_0. Therefore, within the limits of accuracy imposed by the present data, the phonon mean free paths for all the neon samples have the same functional dependence on T/Θ_0. This supports the concept that the Debye temperature is a valid quantity with which to parametrize the volume dependence of thermal-transport phenomena in simple dielectric solids.

Also illustrated in Fig. 3 are the mean free paths obtained from the $\simeq$1 bars conductivity measurements of

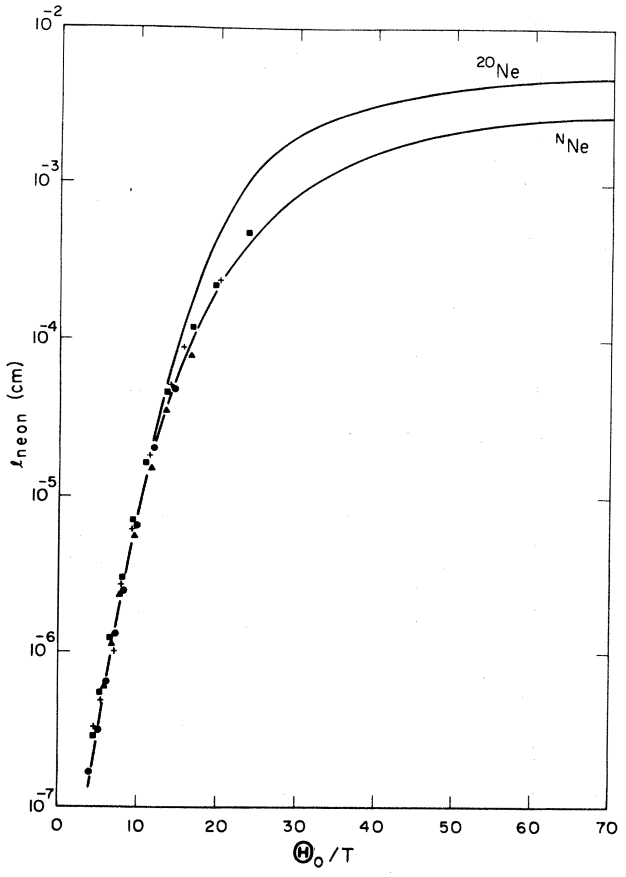

FIG. 3. Computed phonon mean free paths for the neon samples as a function of Θ_0/T. The data are identified by the same plotting symbols as in Fig. 2. Free paths obtained from the results of Kimber and Rogers (Ref. 7) for natural neon ^{N}Ne and pure ^{20}Ne are represented by the lower and upper solid lines, respectively.

Kimber and Rogers[7] on natural neon ^{N}Ne and nominally pure ^{20}Ne (containing $\lesssim$0.05 at.% ^{22}Ne). The latter curve is included to demonstrate the effect of the relative content of ^{22}Ne at low temperatures. Indeed, it is clear that at the lowest temperatures attained by the above investigators, the presence of only $\simeq$9% of this atomic species in natural neon is sufficient to reduce l by nearly a factor of 2.

Furthermore, it appears from Fig. 3 that only for values of $\Theta_0/T \lesssim 12$ does the contribution of the ^{22}Ne isotopic lattice distortions to the scattering of phonons begin to become relatively insignificant. It is in this temperature range, then, that the dissipative interactions of the phonons among themselves are expected to be the dominant factor limiting the free path l. These are the umklapp processes, for which wave vector is conserved only up to an additive constant equal to a nonzero reciprocal-lattice vector G. Such interactions may be viewed as inelastic phonon-phonon collisions by which wave-vector momentum $\hbar G$ is extracted from the momentum current distribution of the phonon gas and transferred to the crystal lattice, thereby attenuating the flow of heat. Those phonon interactions (normal processes), which satisfy the wave-vector selection rule with $G=0$, conserve momentum and need not be considered in the calculation of the phonon free path.

The functional form of the free path at these moderate temperatures, where three-phonon events are expected to play a principal role, is suggested by the work of Peierls.[14] Implicit in his treatment of the problem is the supposition that l should be inversely proportional to the number of phonons which can participate in resistive umklapp processes. Such phonons have wave vectors that extend halfway or more out to the edge of the first Brillouin zone and therefore have energies of greater than approximately $\hbar\omega_q(\max)/2$, or equivalently $k_B\Theta/b$, where $k_B\Theta$ denotes the maximum quantum energy that can be excited among the lattice modes and $b \lesssim 2$. Thus, because they are Bose particles, with statistical mechanics requiring the population n_q of any mode with wave vector q to be close to the equilibrium Planck distribution

$$[\exp(\hbar\omega_q/k_BT)-1]^{-1} ,$$

then the number of phonons suitable for umklapp scattering is roughly

$$[\exp(\Theta/bT)-1]^{-1} ,$$

so that the mean free path should vary as the reciprocal of this expression. Consequently, if Θ_0 is again used to scale the temperature, it seems appropriate to fit the data below $\Theta_0/T=12$ in Fig. 3 with the formula

$$l = a[\exp(\Theta_0/bT)-1] . \quad (5)$$

Utilizing a nonlinear least-squares technique to optimize the fitting parameters, it is found that $a=2.36\times10^{-8}$ cm and $b=1.68$ yield the best representation of the umklapp-limited data in terms of Eq. (5). The resulting fitting curve is excellent in that the experimental points are randomly distributed about it with an 11% average deviation, which is of the same order as the pre-

cision of the measurements themselves.

It is likewise encouraging to note that the value of 1.68 obtained for b is consistent with the prediction made by Peierls that it be less than approximately 2. In fact, the agreement is quite satisfactory in view of the approximate nature of Peierls's estimate, since this parameter is sensitive to the details of the geometry of the frequency dispersion surfaces throughout the Brillouin zone. Furthermore, this same value of b adequately describes the data for each of the neon samples. The reason for this can be understood in terms of the recent inelastic neutron scattering studies on neon, which indicate all the vibrational modes scale with compression by very nearly the same factor; i.e., the shape of the phonon density-of-states distribution is practically independent of v.[11] It is also reassuring that analogous data for solid argon[15] are best fit with essentially the same value of b as for neon (see Table II) in accordance with these two rare-gas solids having similar intermolecular forces and phonon spectra.[16]

Just as b gives some measure of the threshold energy required by the phonons to partake in umklapp processes, the other adjustable parameter a in Eq. (5) is related to the strength with which such lattice waves couple. For instance, smaller values of a signify a greater degree of interaction between the phonons, which in turn implies a more anharmonic interatomic potential. Quantitatively, a generalization of the work of Kontorova[17] suggests the following relation between a and an assumed central interatomic pair potential $U(r)$:

$$a \simeq \sigma(U'')^3/k_B\Theta(U''')^2 . \tag{6}$$

Here, U'' and U''', respectively, represent the second and third derivatives of the potential evaluated at the position $r=\sigma$ of the minimum $-\epsilon$ of its attractive well. With the interaction potential for neon and argon expressed in the common functional form $U(r)=\epsilon f(r/\sigma)$, the above formula reduces to

$$a \simeq \sigma/\Lambda , \tag{7}$$

where use has also been made of the fact that $k_B\Theta \simeq \hbar(U''/M)^{1/2}$ for atoms of mass M arranged in an fcc structure and subject to nearest-neighbor interactions only.[18] The denominator Λ in this relation for a is simply the dimensionless parameter $2\pi\hbar(\sigma^2 M\epsilon)^{-1/2}$ introduced by DeBoer[19] as a measure of quantum-mechanical deviations from the classical principle of corresponding states. In terms of a Lennard-Jones 6-12 potential, it follows from Eq. (7) that

$$(a_{\mathrm{Ne}}/a_{\mathrm{Ar}})_{\mathrm{theory}}=0.26$$

when the values of σ and ϵ listed by Horton[20] are employed. This result, not unexpectedly, predicts a low-temperature anharmonicity of solid neon which is somewhat greater than that for argon. Here again, experiment correlated quite well with theory since the numbers listed in Table II yield

$$(a_{\mathrm{Ne}}/a_{\mathrm{Ar}})_{\mathrm{expt}}=0.23 .$$

TABLE II. Best values for the adjustable parameters of the formula $l=a[\exp(\Theta_0/bT)-1]$ used to fit the mean-free-path data in the ranges $3.95 \leq (\Theta_0/T)_{\mathrm{Ar}} \leq 13.24$ and $3.75 \leq (\Theta_0/T)_{\mathrm{Ne}} \leq 11.24$.

	a	b
Argon	10.2×10^{-8} cm	1.66
Neon	2.36×10^{-8} cm	1.68

VI. MORE FUNDAMENTAL THEORETICAL CONSIDERATIONS

Although the description of heat transport due to Peierls is useful for the analysis of experimental results, it is, in a sense, not entirely complete. Indeed, the very parameters whose adjustment allow for good fits of the data are available for this purpose only because the phenomenological formulation is unable to specify their values quantitatively. Nevertheless, semi-empirical approaches such as this are heavily relied upon chiefly because there is, as yet, no widely applicable self-contained theory of lattice thermal conduction.

Of the few attempts to develop an accurate prediction of κ from first principles,[21-24] the effort by Julian[23] is by far the most ambitious. He assumed a Boltzmann-type transport equation for determining the steady-state phonon distribution and dealt solely with the case in which the collision term is governed by three-phonon scattering events. Giving special attention to the rare-gas crystals, he then derived an expression from which the conductivity's absolute dependence on temperature and volume can be directly computed.

With the use of only the appropriate interatomic potential and atomic mass as input to distinguish between neon, argon, krypton, and xenon, it is a straightforward matter to follow Julian's prescription and numerically evaluate $\kappa(T,v)$ for any one of the rare gases. In the case of neon, a realistic mathematical model for the intermolecular forces has been given by Goldman and Klein.[25] It entails a Morse function for the repulsive wall and bowl of the interaction energy, as well as van der Waals terms for the long-range tail, with the two portions joined by a spline curve. The specific form of this potential, derived from an analysis of solid-state data incorporating three-body forces, yields theoretical heat-capacity values in excellent agreement with the measurements of Fugate and Swenson[6] and is therefore assumed well suited for the present calculations.

The resulting conductivity is displayed as a function of molar volume at constant reduced temperature in Fig. 4. The particular value $T/\Theta_0=\frac{1}{8}$ is chosen for the construction of this graph because it is common to the umklapp-dominated regime of each of the neon samples and thereby facilitates comparison between theory and the experimental results which it is intended to simulate. Unfortunately, as the figure makes clear, Julian's findings are in serious disagreement with the data, being low in magnitude by a factor which becomes as large as about 4 or 5 at low densities.

Matters were subsequently improved somewhat by Benin,[26] who carefully reanalyzed Julian's work within the

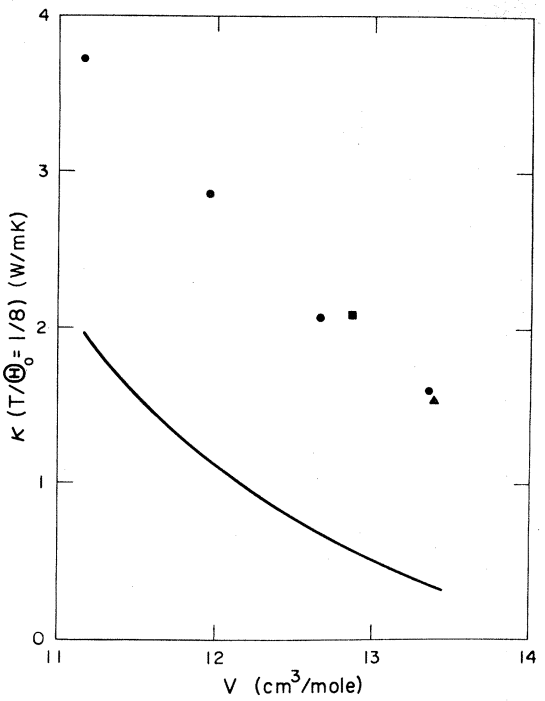

FIG. 4. Volume dependence of the thermal conductivity of solid neon at the reduced temperature $T/\Theta_0 = 1/8$. The solid line is the prediction of Julian's theory (Ref. 23) and the individually plotted points are empirical data derived from ▲ Kimber and Rogers (Ref. 7), ■ Clemens, sample no. 10 (Ref. 3), and ● present work.

framework of self-consistent phonon theory. Disappointedly, however, the resulting conductivity for neon, calculated at its saturated vapor pressure density, is only about 50% larger than that obtained by Julian. Furthermore, this correction is presumably even less at the smaller molar volumes, where the effects of the zero-point motion of the atoms diminish in importance. Thus, despite its sophistication, the self-consistent phonon approach apparently does little more than to change the qualitative shape of the theoretical curve shown in Fig. 4; the absolute magnitude of κ(theory), although slightly improved, still remains significantly below that of the observed data. It should be noted that any systematic inaccuracies that could be introduced because of less-than-perfect sample quality would, if anything, depress the measured values of κ and therefore cannot serve to justify the discrepancy between theory and experiment.

VII. DIRECTIONS FOR FUTURE WORK

The shortcoming of the theory, as discussed above, is by no means peculiar to neon but has also been noted for argon,[2] thereby strongly indicating the presence of an underlying flaw in the model. Benin himself suggests that the culprit may be the so-called Ziman limit,[27] in whose context Julian's as well as his own previous analysis were performed. Here, umklapp processes are taken to be sufficiently infrequent at low temperatures that the desired solution of the phonon Boltzmann equation differs only little from that which arises when such processes are completely absent. In this way, normal processes alone are assumed to determine the manner by which the energy transported through the crystal is shared among the phonons.

However, Benin gives evidence that this theoretical limit is, in no case, actually realized. Pointing out that umklapp processes never become entirely frozen out, he argues that even at the lowest temperatures they compete with the normal processes in influencing the distribution of energy among the lattice modes. Therefore, whereas all prior treatments of the problem concerned themselves principally with thermal phonons, more recent insights have led Benin to equally emphasize the importance of those few high-energy ($\hbar\omega_q \gg k_B T$) excitations always present to undergo umklapp scattering. Incorporating their special role into a variational calculation of the thermal conductivity and then focusing upon lithium fluoride and sodium fluoride, he did in fact manage to obtain excellent agreement with experiment. Likewise, it is anticipated that application of this concept to the solid rare gases will be successful in greatly reducing the disparity between κ(theory) and κ(experiment) which still exists for these substances.

A promising alternative means for improving the present theoretical results appears to be along the lines of linear-response theory.[28–30] In such an approach, the heat-transport process is formalized not by way of a phonon Boltzmann equation, but rather in terms of an energy current autocorrelation function. Since it is a measure of the response of a system when driven by a small applied temperature field, this function is directly related to the coefficient of thermal conductivity. However, the difficulties entailed in its evaluation presently rival those inherent to the successful solution of the Boltzmann equation. Because of this, little has been achieved in the way of explicit numerical computations. Yet the success with which Werthamer and Chui implemented the correlation function formulation to calculate the three-phonon umklapp thermal relaxation time[31,32] is promising. Just as their work helped explain the observed thermal conductivity of hcp helium, one may be optimistic that further quantitative progress will be forthcoming for the heavier rare-gas solids.

ACKNOWLEDGMENTS

It is a pleasure for the authors to acknowledge support by the National Science Foundation for that portion of this work performed at the University of Delaware under Grants Nos. GP-7739, GH-32491, DMR-78-01307, and DMR-81-00660.

[1]W. D. Seward, D. Lazarus, and S. C. Fain, Jr., Phys. Rev. 178, 345 (1969).
[2]F. Clayton and D. N. Batchelder, J. Phys. C 6, 1213 (1973).
[3]J. E. Clemens, Phys. Rev. B 15, 1072 (1977).
[4]R. K. Crawford and W. B. Daniels, J. Chem. Phys. 55, 5651 (1971).
[5]M. S. Anderson, R. Q. Fugate, and C. A. Swenson, J. Low Temp. Phys. 10, 345 (1973).
[6]R. Q. Fugate and C. A. Swenson, J. Low Temp. Phys. 10, 317 (1973).
[7]R. M. Kimber and S. J. Rogers, J. Phys. C 6, 2279 (1973).
[8]G. K. White and S. B. Woods, Philos. Mag. 3, 785 (1958).
[9]J. A. Leake, W. B. Daniels, J. Skalyo, Jr., B. C. Frazer, and G. Shirane, Phys. Rev. 181, 1251 (1969).
[10]J. Skalyo, Jr., V. J. Minkiewicz, G. Shirane, and W. B. Daniels, Phys. Rev. B 6, 4766 (1972).
[11]J. Eckert, W. B. Daniels, and J. D. Axe, Phys. Rev. B 14, 3649 (1976).
[12]J. M. Ziman, *Principles of the Theory of Solids* (Cambridge University Press, London, 1965).
[13]*Landolt-Börnstein Zahlenwerte und Funktionen aus Physik, Chemie, Astronomie, Geophysik, und Technik* (Springer, Berlin, 1961), Band II, Teil 4.
[14]R. E. Peierls, Ann. Physik 3, 1055 (1929).
[15]H. T. Weston, Ph.D. thesis, Princeton University, Princeton, New Jersey (1976).
[16]Y. Endoh, G. Shirane, and J. Skalyo Jr., Phys. Rev. B 11, 1681 (1975).
[17]T. A. Kontorova, Zh. Tekh. Fiz. 26, 2021 (1956) [Sov. Phys.—Tech. Phys. 1, 1959 (1957)].
[18]C. Domb and L. Salter, Philos. Mag. 43, 1083 (1952).
[19]J. DeBoer, Physica 14, 139 (1948).
[20]G. K. Horton, Am. J. Phys. 36, 93 (1968).
[21]G. Leibfried and E. Schlömann, Nachr. Akad. Wiss. Göttingen, Math. Physik Kl. IIa, 71 (1954).
[22]G. Leibfried, in *Handbuch der Physik,* edited by S. Flügge (Springer, Berlin, 1955), Band VII, Teil 1.
[23]C. L. Julian, Phys. Rev. 137, A128 (1965).
[24]B. I. Bennett, Solid State Commun. 8, 65 (1970).
[25]V. V. Goldman and M. L. Klein, J. Low Temp. Phys. 12, 101 (1973).
[26]D. B. Benin, Phys. Rev. Lett. 20, 1352 (1968).
[27]D. Benin, Phys. Rev. B 5, 2344 (1972).
[28]J. Ranninger, Ann. Phys. (N.Y.) 45, 452 (1967).
[29]J. Ranninger, Ann. Phys. (N.Y.) 49, 297 (1968).
[30]J. Ranninger, J. Phys. C 2, 640 (1969).
[31]N. R. Werthamer and S.-T. Chui, Solid State Commun. 10, 843 (1972).
[32]N. R. Werthamer and S.-T. Chui, Phys. Lett. 41A, 157 (1972).